J|A|C|S ARTICLES

Published on Web 01/25/2010

Structure and Excitonic Coupling in Self-Assembled Monolayers of Azobenzene-Functionalized Alkanethiols

Cornelius Gahl,*,† Roland Schmidt,†,‡ Daniel Brete,†,‡ Erik R. McNellis,§ Wolfgang Freyer,† Robert Carley,† Karsten Reuter,§ and Martin Weinelt*,†,‡

Max-Born-Institut, Max-Born-Str. 2A, 12489 Berlin, Germany, Freie Universität Berlin, Fachbereich Physik, Arnimallee 14, 14195 Berlin, Germany, and Fritz-Haber-Institut der Max-Planck-Gesellschaft, Faradayweg 4-6, 14195 Berlin, Germany

Received May 13, 2009; E-mail: gahl@mbi-berlin.de; weinelt@mbi-berlin.de

Abstract: Optical properties and the geometric structure of self-assembled monolayers of azobenzene-functionalized alkanethiols have been investigated by UV/visible and near edge X-ray absorption fine structure spectroscopy in combination with density-functional theory. By attaching a trifluoro-methyl end group to the chromophore both the molecular tilt and twist angle of the azobenzene moiety are accessible. Based on this detailed structural analysis the energetic shifts observed in optical reflection spectroscopy can be qualitatively described within an extended dipole model. This substantiates sizable excitonic coupling among the azobenzene chromophores as an important mechanism that hinders *trans* to *cis* isomerization in densely packed self-assembled monolayers.

Introduction

The functionalization of surfaces with molecular switches is a rapidly growing field in today's research. Molecules can be used as repeatable building blocks for electronics and sensors and thereby open the perspective for tailoring devices on the nanoscale.[1−6] In this respect self-assembled monolayers (SAMs) have often been considered as ideal platforms to order and align molecules at surfaces.[7,8] For this purpose the combination of aliphatic and aromatic molecules is widely proposed as a versatile class of systems to control structure and energetics within the SAM. An alkanethiol is used as a linker, which binds with its sulfur headgroup to a metal template, typically a gold surface. The alkyl-chain spacer carries the aromatic entity as an end group. The supramolecular architecture of the SAM is ruled by the balance of adsorbate−substrate and adsorbate−adsorbate interactions. This comprises the bond strength and bond angle between sulfur and substrate atoms as well as intermolecular couplings within the densely packed layer.[9] The latter involve van der Waals and electrostatic interactions among both aliphatic spacers and aromatic headgroups. In recent years biphenyl carrying alkanethiols have been extensively investigated by core-level spectroscopies and scanning probe techniques, and SAMs with a high degree of molecular orientation and lateral order have been achieved.[9−11]

However, to functionalize SAMs with molecular switches, such as azobenzene units, it is not only crucial to tailor the molecular structure but also even more important to control the coupling of the chromophore to its environment. In most investigations of molecular switches at surfaces, the electronic coupling strength to the substrate is taken care of by various spacer groups.[6−12] In a SAM, however, neighboring molecular switches can influence each other by steric hindering as well as electronic and excitonic coupling. This may influence the molecular motion and/or electronic structure and thereby hinder or promote functionality by cooperative action.[13−15]

Azobenzene linked to a Au(111) surface by an alkanethiol is known to form well-ordered SAMs with a surface area of 0.24−0.26 nm^2 per molecule.[16,17] Steric hindrance within these densely packed structures is mainly assumed to be the reason why photoisomerization has commonly not been observed.[18,19]

Various efforts have been made to increase the spacing between the switching moieties or modify their mutual orienta-

† Max-Born-Institut.
‡ Freie Universität Berlin.
§ Fritz-Haber-Institut der MPG.

(1) Bryce, M. R.; Petty, M. C.; Bloor, D. *Molecular Electronics*; Oxford University Press: New York, 1995.
(2) Joachim, C.; Gimzewski, J. K.; Aviram, A. *Nature* **2000**, *408*, 541–548.
(3) Feringa, B. L. *Molecular Electronics*; Wiley: Weinheim, 2001.
(4) Zhu, X. Y. *Surf. Sci. Rep.* **2004**, *56*, 1–83.
(5) Katsonis, N.; Kudernac, T.; Walko, M.; van der Molen, S. J.; van Wees, B. J.; Feringa, B. L. *Adv. Mater.* **2006**, *18*, 1397–1400.
(6) Katsonis, N.; Lubomska, M.; Pollard, M. M.; Feringa, B. L.; Rudolf, P. *Prog. Surf. Sci.* **2007**, *82*, 407–434.
(7) Zharnikov, M.; Grunze, M. *J. Phys.: Condens. Mater.* **2001**, *13*, 11333–11365.
(8) Bent, S. F. *ACS Nano* **2007**, *1*, 10–12.
(9) Cyganik, P.; Buck, M.; Strunskus, T.; Shaporenko, A.; Wilton-Ely, J. D. E. T.; Zharnikov, M.; Wöll, C. *J. Am. Chem. Soc.* **2006**, *128*, 13868–13878.
(10) Cyganik, P.; Buck, M.; Azzam, W.; Wöll, C. *J. Phys. Chem. B* **2004**, *108*, 4989–4996.
(11) Cyganik, P.; Buck, M.; Wilton-Ely, J. D. E. T.; Wöll, C. *J. Phys. Chem. B* **2005**, *109*, 10902–10908.
(12) Wolf, M.; Tegeder, P. *Surf. Sci.* **2009**, *603*, 1506–1517.
(13) Pace, G.; Ferri, V.; Grave, C.; Elbing, M.; von Hanisch, C.; Zharnikov, M.; Mayor, M.; Rampi, M. A.; Samori, P. *Proc. Natl. Acad. Sci. U.S.A.* **2007**, *104*, 9937–9942.
(14) Elbing, M.; Blaszczyk, A.; von Hänisch, C.; Mayor, M.; Violetta, F.; Grave, C.; Rampi, M. A.; Pace, G.; Samorì, P.; Shaporenka, A.; Zharnikov, M. *Adv. Funct. Mater.* **2008**, *18*, 2972–2983.
(15) Weiss, P. S. *Acc. Chem. Res.* **2008**, *41*, 1772–1781.

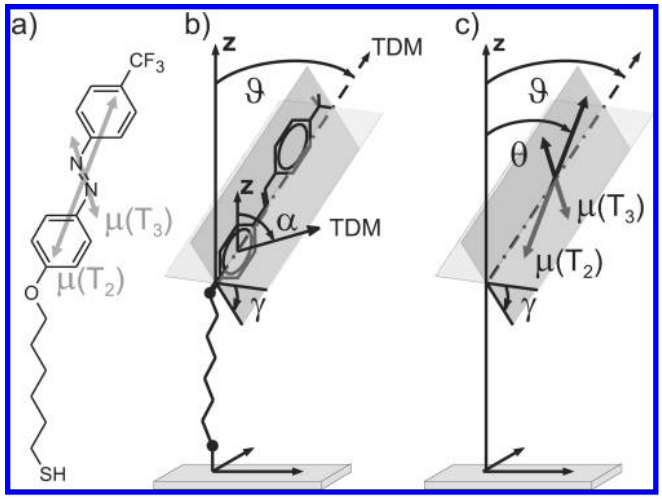

Figure 1. (a) Structural formula of the azobenzene alkanethiol TF-Az6. In Az6 the trifluoro-methyl group (CF_3) is replaced by a hydrogen atom. The gray double arrows indicate the optical transition dipole moments $\mu(T_2)$ and $\mu(T_3)$ probed in UV/vis spectroscopy. Their orientation with respect to the molecular framework is obtained from a TD-DFT calculation. They are coplanar to the plane of the *trans* isomer but tilted with respect to the C−CF_3 axis by 8.5° and 46.7°, respectively. (b) The sketch of the molecule indicates the geometric structure and the angles ϑ and γ used to describe the orientation of the azobenzene moiety. The angles α and ϑ describe the mean tilt angles of the NEXAFS-TDMs probed in C 1*s* core-level excitation with respect to the surface normal *z* (see text). (c) Illustration of the tilt angle $\theta = \theta(\vartheta, \gamma)$ of the optical TDMs compared to the molecular tilt and twist angle (shown is the angle θ of the optical TDM $\mu(T_2)$; an equivalent angle can be defined for $\mu(T_3)$).

tion in the SAM.[13,14,20] In addition, molecular switches isolated in a passive SAM matrix or at defects have been studied and switched by light.[15,21] While these experiments underscore the importance of steric hindrance, the local field enhancement near an STM tip nevertheless enables optical switching even in densely packed SAMs, so that photoisomerization cannot be entirely inhibited by steric constraints.[22] However, the full mechanism behind the observed quenching is to date not understood, and the grand goal to functionalize surfaces by reproducible switching of the entire SAM remains elusive.

In the present contribution we show that azobenzene chromophores in a close-packed structure influence each other strongly by excitonic coupling. This leads to energetic shifts and narrowing of optical absorption lines. We deduce in detail the molecular orientation of azobenzene-functionalized alkanethiols within well-ordered SAMs from near-edge X-ray absorption fine structure (NEXAFS) measurements in combination with density-functional theory (DFT) calculations. On this basis we model the shifts observed in the UV/visible (UV/vis) spectra within the framework of the extended dipole model.[23] Excitonic coupling and the concomitant fast delocalization of the excitation within the SAM is expected to contribute strongly to the suppression of the photoisomerization reaction. This detailed insight into the intermolecular coupling denotes a step forward in developing a design of SAMs containing molecular switches with proper functionality.

Methods

Chemicals and Sample Preparation. 6-[(4-Phenylazo)phenoxy]-hexane-1-thiol and 6-[(4-trifluoromethylphenylazo)phenoxy]hexane-1-thiol have been synthesized and purified as described elsewhere.[24] In the following the molecules are referred to as Az6 and TF-Az6. The structural formula, the relative orientation of the optical and NEXAFS transition dipole moments (TDM), and the angles defining the molecular orientation on the surface are given in Figure 1.

Commercially available 300 nm Au films on mica, which were annealed after gold deposition, serve as substrates for SAM formation. The polycrystalline surface exhibits large Au(111) terraces of a few hundred nm^2.[25] Preexisting carbon and sulfur contamination of the gold surface is largely eliminated within the self-assembly process. This has been routinely verified by recording S 2*p* X-ray photoelectron spectra (XPS).[7,24] SAMs are prepared by immersing the gold-covered mica substrates in 0.1 mM ethanolic solution of Az6 and TF-Az6 for 24 h at room temperature. To avoid weakly bound molecules residing on top of the SAM, the samples were rinsed thoroughly with pure ethanol, dried in a flow of argon gas, and immediately transferred into the ultrahigh-vacuum (UHV) system for core-level spectroscopy or the optical spectrometer for UV/vis spectroscopy in reflection.

X-ray and UV/Vis Spectroscopy. NEXAFS spectroscopy and XPS experiments were carried out at beamline U41-PGM of the storage ring BESSY II (Helmholtz-Zentrum Berlin). We use a two-chamber UHV system equipped with a fast sample transfer system and a hemispherical electron analyzer with a five-channel detector (Omicron EA125). In NEXAFS spectroscopy Auger electrons were recorded in the direction perpendicular to the polarization of the exciting X-ray beam. This lowers the intensity of direct photoemission and enhances the surface sensitivity. To reduce radiation damage, the sample was kept at liquid nitrogen temperature and a fast shutter was used to block the beam during the scan of the monochromator and undulator.[26] The shutter is equipped with a GaAs photodiode, which records the X-ray flux alternatingly with the measurement and is used to normalize the NEXAFS spectrum. Using the shutter the total exposure for a single NEXAFS scan is reduced to 10^{16} photons/cm^2, a fluence for which negligible C−H bond breaking is reported in the literature.[26] The sample can be rotated around the X-ray-beam axis in order to determine the polarization dependence for a fixed angle of incidence of $\beta = 20°$ with respect to the surface plane. The degree of polarization of the synchrotron radiation *P* at the U41-PGM is expected to be 96 ± 2%.[27]

For UV/vis spectroscopy a scanning double monochromator Perkin-Elmer Lambda 900 spectrometer was used. The spectra of the SAMs on Au/mica were measured in reflection mode with

(16) (a) Wolf, H.; Ringsdorf, H.; Delamarche, E.; Takami, T.; Kang, H.; Michel, B.; Gerber, C.; Jaschke, M.; Butt, H.-J.; Bamberg, E. *J. Phys. Chem.* **1995**, *99*, 7102–7107. (b) Jaschke, M.; Schönherr, H.; Wolf, H.; Butt, H.-J.; Bamberg, E.; Besocke, M. K.; Ringsdorf, H. *J. Phys. Chem.* **1996**, *100*, 2290–2301.
(17) Mannsfeld, S. C. B.; Canzler, T. W.; Frith, T.; Proehl, H.; Leo, K.; Stumpf, S.; Goretzki, G.; Gloe, K. *J. Phys. Chem. B* **2002**, *106*, 2255–2260.
(18) Wang, Z.; Nygard, A.-M.; Cook, M. J.; Russell, D. A. *Langmuir* **2004**, *20*, 5850–5857.
(19) Caldwell, W. B.; Campbell, D. J.; Chen, K.; Herr, B. R.; Mirkin, C. A.; Malik, J.; Durbin, M. K.; Dutta, P.; Huangt, K. G. *J. Am. Chem. Soc.* **1995**, *117*, 6071–6082.
(20) Suda, M.; Kameyama, N.; Ikegami, A.; Einaga, Y. *J. Am. Chem. Soc.* **2008**, *131*, 865–870.
(21) Kumar, A. S.; Ye, T.; Takami, T.; Yu, B.-C.; Flatt, A. K.; Tour, J. M.; Weiss, P. S. *Nano Lett.* **2008**, *8*, 1644–1648.
(22) Micheletto, R.; Yokokawa, M.; Schroeder, M.; Hobara, D.; Ding, Y.; Kakiuchi, T. *Appl. Surf. Sci.* **2004**, *228*, 265–270.
(23) Kuhn, H.; Kuhn, C. In *J-Aggregates*; Kobayashi, T., Ed.; World Scientific: 1996; pp 1−40.
(24) Schmidt, R.; McNellis, E.; Freyer, W.; Brete, D.; Gieβel, T.; Gahl, C.; Reuter, K.; Weinelt, M. *Appl. Phys. A* **2008**, *93*, 267–275.
(25) Kowalczyk, P. *Appl. Surf. Sci.* **2007**, *253*, 4036–4040.
(26) Feulner, P.; Niedermeyer, T.; Eberle, K.; Schneider, R.; Menzel, D.; Baumer, A.; Schmich, E.; Shaporenko, A.; Tai, Y.; Zharnikov, M. *Phys. Rev. Lett.* **2004**, *93*, 178302−1–4.
(27) Jung, C.; Eggenstein, F.; Hartlaub, S.; Follath, R.; Schmidt, J. S.; Senf, F.; Weiss, M. R.; Zeschke, T.; Gudat, W. *Nucl. Instrum. Methods Phys. Res., Sect. A* **2001**, *467*, 485–487.

unpolarized light at an angle of incidence of 45°. The SAM-induced change in reflectivity is derived from the difference between the reflectivity of the gold substrate before and after SAM preparation. Thereby we obtain the complete contribution of the molecules in the SAM to the UV/vis spectrum. This is in contrast to the commonly evaluated difference of spectra before and after illumination which is sensitive only to those molecules which have been optically switched and may thus represent a minority species.

Density-Functional Theory Calculations. To support the experimental data analysis, DFT and time-dependent DFT (TD-DFT) calculations were performed using the Gaussian suite of programs,[28] the B3LYP hybrid density functional[29] to treat electronic exchange and correlation, and the all-electron def-TZVP basis set.[30] Excitation energies and transition dipole moments of low lying resonances in the UV spectrum were computed within the response theory formulation of TD-DFT,[31] using the B3LYP functional in the adiabatic approximation.[32] Neglecting the effect of the underlying substrate and the surrounding molecules in the SAM, the calculations focused on single Az6 and TF-Az6 units with a six-unit alkanethiol chain as illustrated in Figure 1a.

Results

Molecular Orientation. Concerning the relation between structure and function of the photoswitch in the SAM it is essential to determine the orientation of the azobenzene moiety, especially the π-conjugated system of the phenyl rings and the long molecular axis. They have been extracted from the polarization dependence of the C 1*s* and N 1*s* to π^* and the C 1*s* to $\sigma^*(C-CF_3)$ transitions in NEXAFS spectroscopy. Corresponding spectra of TF-Az6 SAMs on gold on mica are shown in Figure 2a and b for the C 1*s* and N 1*s* edges, respectively. They have been recorded for *s*- and *p*-polarization of the X-ray beam with a photon-energy resolution of 0.1 eV. Spectra are aligned at the pre-edge below the first transition and well above the ionization threshold, where no significant resonances are observed and the measured signal can be assumed to be independent of the molecular orientation.

Overall the NEXAFS spectra exhibit a pronounced dependence of the Auger yield on the polarization of the exciting X-ray radiation, which is a clear signature of a high degree of molecular orientation within the SAM.[33] The spectra are dominated by absorption from the azobenzene moiety since the Auger signal of the alkyl chain buried beneath the chromophore is damped.[34,35]

At the carbon edge the dominant peak at ~285.7 eV corresponds to the transition from the C 1*s* to π^* (LUMO, lowest unoccupied molecular orbital). This orbital extends over the two phenyl rings as well as the azo group. The width of the C 1*s* to π^* (LUMO) transition of 1.4 eV and its three-peak structure are attributed to the distinct chemical shifts of the C 1*s* core level in the different environments, i.e. the phenyl ring, and the carbon atoms bound to the azo-, phenoxy-, and the trifluoromethyl groups (C═C, C—N, C—O, $C-CF_3$).[24] At the nitrogen edge this π^* resonance is found at 399.0 eV and exhibits a smaller line width of 0.4 eV. From the strong polarization contrast the mean tilt angle α of the 1*s* to π^* transition dipole moment in TF-Az6 is determined as $\alpha_{C1s} = 75 \pm 3°$ and $\alpha_{N1s} = 77 \pm 3°$ according to

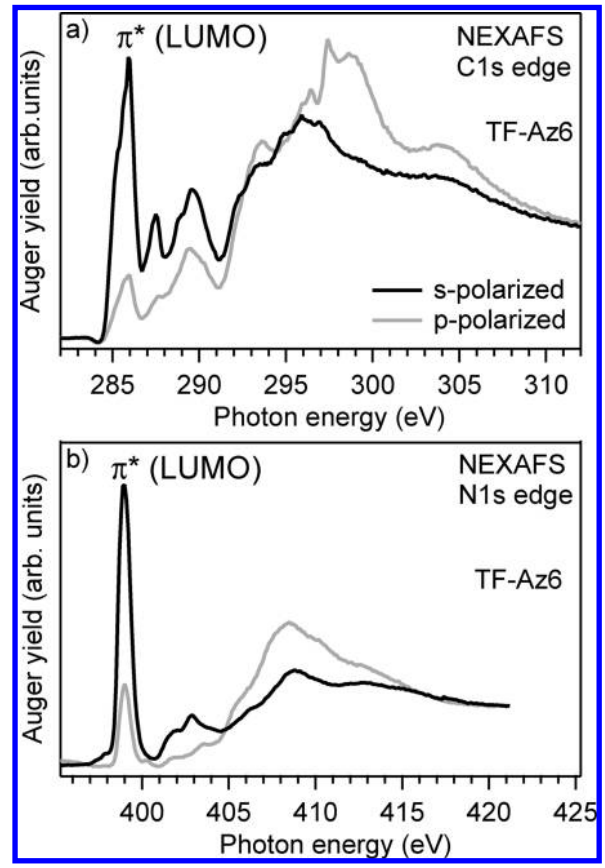

Figure 2. NEXAFS spectra of TF-Az6 at the (a) C1*s* and (b) N1*s* absorption edge. The sample was rotated around the X-ray beam axis at a fixed angle of incidence of $\beta = 20°$ with respect to the surface plane. For *p*- and *s*-polarization the field vector was parallel and perpendicular, respectively, to the plane of incidence.

$$\sin^2\alpha = \left(1 - \frac{1}{2}\tan^2\beta - \frac{1}{2\cos^2\beta}\frac{1 - P - PI}{P - (1 - P)I}\right)^{-1} \qquad (1)$$

Equation 1 is valid for vector-like orbitals in the case of 3-fold or higher symmetry.[36] Herein α denotes the angle between the vector-like π^* orbital and the surface normal (cf. Figure 1b), and $\beta = 20°$ describes the fixed angle of incidence of the X-ray beam relative to the surface plane. $P = 0.96$ is the degree of polarization of the X-ray beam, and I is the measured intensity ratio of the π^* absorption peak for *s*- vs *p*-polarization. NEXAFS spectroscopy is a local probe of the electronic structure, since the dipole transition projects the wave function of the unoccupied valence orbital onto the core hole. Thus for the C 1*s* and N 1*s* core holes we probe the atomic 2*p* contributions to the molecular valence orbitals, which define the orientation of the transition dipole moments in NEXAFS (TDM in Figure 1b).[33] Correspondingly, the comparable angles α_{N1s} and α_{C1s} of the 1*s* to π^* transition-dipole moments for excitation at the azo group (N1*s*) and the phenyl rings (C1*s*) clearly indicate that

(28) Frisch, M. J.; et al. *Gaussian 03*, revision B.05; Gaussian, Inc.: Pittsburgh, PA, 2003.
(29) Stephens, P. J.; Devlin, F. J.; Chabalowski, C. F.; Frisch, M. J. *J. Phys. Chem.* **1994**, *98*, 11623–11627.
(30) Schäfer, A.; Huber, C.; Ahlrichs, R. *J. Chem. Phys.* **1994**, *100*, 5829–5835.
(31) Casida, M. E.; Jamorski, C.; Casida, K. C.; Salahub, D. R. *J. Chem. Phys.* **1998**, *108*, 4439–4449.
(32) Bauernschmitt, R.; Ahlrichs, R. *Chem. Phys. Lett.* **1996**, *256*, 454–464.
(33) Stöhr, J. *NEXAFS Spectroscopy*; Springer Series in Surface Sciences 25; Springer: corrected printing 1996.
(34) Hähner, G.; Kinzler, M.; Wöll, C. T. C.; Grunze, M. *J. Vac. Sci. Technol. A* **1992**, *10*, 2758–2763.
(35) Lamont, C. L. A.; Wilkes, J. *Langmuir* **1999**, *15*, 2037–2042.
(36) Stöhr, J.; Outka, D. A. *Phys. Rev. B* **1987**, *36*, 7891–7905.

the azobenzene moiety favors the *trans* conformation in thermal equilibrium. According to our DFT calculations and in analogy to NEXAFS of the free benzene molecule,[37] the absorption peaks of the aromatic system in the energy range up to 5 eV above the π^* (LUMO) resonance are assigned to excitations to higher lying π^* orbitals and to mixed C−H valence/Rydberg states with predominantly σ-character. The polarization dependence of the higher lying π^* transitions mimics that of the LUMO resonances and thus corroborates the orientation of the azobenzene moiety, i.e. the tilt angle α determined through the C1*s* and N1*s* to LUMO transition dipole moments.

The transitions at the nitrogen edge at approximately 409 and 414 eV are assigned to σ^* shape resonances. Based on the interrelation of the shape resonance position and the bond length, we assign these resonances to the N−C and N−N bonds, respectively.[33]

In addition to the pronounced π^* transitions, the C1*s* NEXAFS spectra show sharp resonances in the photon energy range of 294 to 300 eV. These absorption features are missing in the NEXAFS spectra of Az6 in Figure 3. They are attributed to excitations involving the chemically shifted C1*s* level of the CF_3 group of TF-Az6 (gray area). In analogy to hexafluoroethane the main resonances are assigned to transitions to the σ^* (C−F) orbitals in the photon energy range of 295−298 eV and to the σ^* (C−C) resonance at 299 eV.[38,39] According to our XPS measurements the C1*s* core level of the trifluoro-methyl group exhibits a chemical shift of 8.0 eV with respect to the carbon atoms of the alkyl chain.[24] Adding this shift to the energy of the σ^* (C−H) resonance of the alkyl chain at ∼287.8 eV we expect σ^* (C−F) resonances at ∼295.8 eV corroborating the above assignment.[7] The polarization dependence of the C1*s* to σ^* (C−C) resonance at the CF_3 group is evaluated relying on the building block scheme; i.e., in the relevant photon energy range the Az6 NEXAFS spectrum contains all but the CF_3 related transitions. For this we assume a comparable orientation of TF-Az6 and Az6 molecules supported by the very similar intensity and polarization dependence of the 1*s* to π^* transition. For the higher-lying bound state resonances, i.e. for photon energies up to 290 eV, we observe changes in the intensity which indicate subtle differences in the molecular orientation and/or a redistribution of oscillator strength upon changing the end group. Nevertheless, the polarization dependence of the π^*-resonance indicates comparable tilt angles α of the azobenzene moiety, and we likewise expect the continuum resonances to be little affected by the different end groups. As depicted in Figure 3b subtraction of both spectra removes the background from the broad carbon shape resonances associated with the phenyl rings. The resulting NEXAFS contrast of 4.3:1 corresponds to a tilt angle ϑ (C−CF_3) = 30° ± 6° (cf. Figure 1b). The larger error bar is due to the uncertainty in the background subtraction and the variation in peak ratios from sample to sample. We note that fluorinated hydrocarbons are extremely sensitive to radiation damage.[24,40] We therefore recorded spectra at BESSY at beamline UE112-PGM1 with reduced flux (not shown) which corroborate the above results.

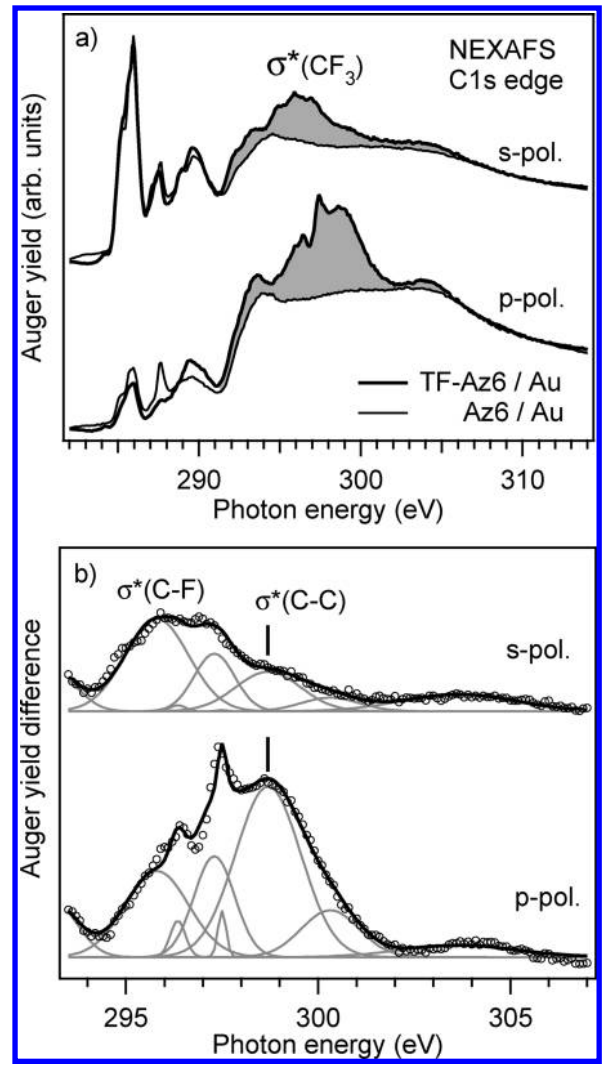

Figure 3. (a) NEXAFS spectra of TF-Az6 and Az6. (b) Difference spectra (gray area in part a) on an enlarged photon energy scale singling out transitions from the chemically shifted C 1*s* core level at the trifluoro-methyl group.

From the measured orientation $\alpha = 76°$ of the 1*s* to π^* transition dipole moments with respect to the surface normal and the tilt angle $\vartheta = 30°$ of the C−CF_3 axis, we can derive the twist angle γ of the azobenzene moiety (cf. Figure 1b) to be 61 ± 10°, using the relation

$$\cos \alpha = \sin \vartheta \cdot \cos \gamma \qquad (2)$$

The twist angle not only influences the mutual interaction between neighboring azobenzene moieties but also impacts the connection between the azobenzene chromophore and the alkyl chain. As depicted in Figure 4a our DFT calculations show that the C−O−C bond angle ξ of 120° is rather rigid with the three atoms lying in the plane of the adjacent phenyl ring ($\chi = 0°$). The phenoxy group is, however, rather freely rotatable around the internal azimuthal angle χ in a range of ±30°. As evident from Figure 4b azobenzene linked directly to the alkyl chain is instead almost freely rotatable around the C−phenyl bond with a shallow potential minimum for an orientation of the alkyl chain perpendicular to the phenyl plane ($\chi = \pm 90°$). The same holds for the intensively studied biphenyl-alkanethiols (BP*n*). Thus if lateral interactions among the chromophores dominate the structure of the SAM, the molecular framework can adjust and

(37) Püttner, R.; Kolczewski, C.; Martins, M.; Schlachter, A. S.; Snell, G.; Sant'Anna, M.; Viefhaus, J.; Hermann, K.; Kaindl, G. *Chem. Phys. Lett.* **2004**, *393*, 361–366.
(38) Ishii, I.; McLaren, R.; Hitchcock, A. P.; Jordan, K. D.; Choi, Y.; Robin, M. B. *Can. J. Chem.* **1988**, *66*, 2104–2121.
(39) Ågren, H.; Carravetta, V.; Vahtras, O.; Pettersson, L. G. M. *Phys. Rev. B* **1995**, *51*, 17848–17855.
(40) Frey, S.; Heister, K.; Zharnikov, M.; Grunze, M. *Phys. Chem. Chem. Phys.* **2000**, *2*, 1979–1987.

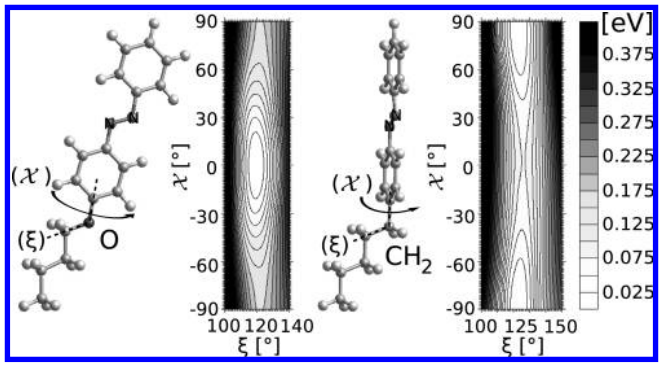

Figure 4. Total energy contour plots for Az6 with the azobenzene chromophore in the *trans* configuration for (a) an oxygen bridge and (b) a carbon bridge between alkanethiol chain and azobenzene chromophore. The stiffness of the bridge is explored by varying the C−O−C bond angle ξ and internal azimuthal angle χ. Identical results have been obtained for TF-Az6.

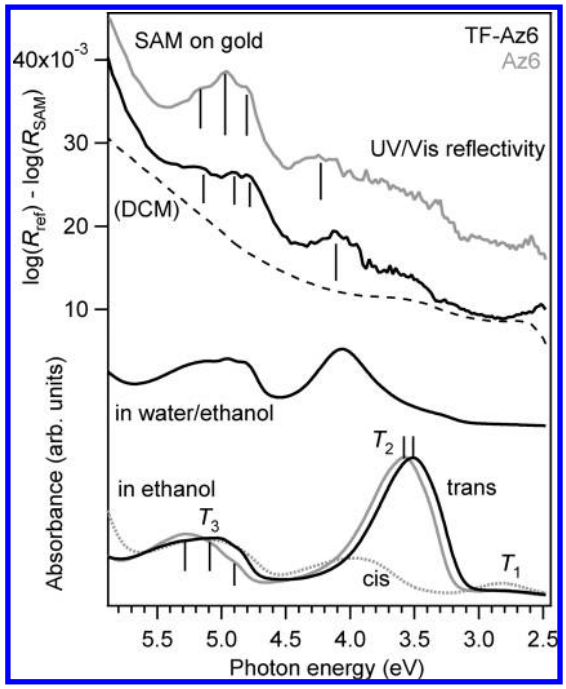

Figure 5. UV/vis absorption spectra of TF-Az6 (black lines) and Az6 (gray lines). The spectra of the SAM (upper lines) have been measured in reflection and are difference spectra of the SAM-covered and clean gold substrate. The dashed line is a dielectric continuum-model (DCM) calculation of the background of the gold substrate (see text). The spectra in solution (lower lines) are recorded in transmission. In ethanol the molecules are solvated as monomers, while in a water/ethanol mixture of 4:1 they form aggregates.[41] The *cis* Az6 isomer was isolated via thin layer chromatography, and the corresponding spectrum is additionally shown as a gray dotted line. All spectra are taken from pristine samples handled only in amber safe light before measuring.

we may find similar orientations of the azobenzene and biphenyl moieties, i.e. tilt and twist angles ϑ and γ in the corresponding SAMs (cf. Figure 1b).

Optical Properties in the UV/Vis Range. Absorption spectra in solution as well as reflection spectra from the SAM for TF-Az6 and Az6 are shown in Figure 5. In ethanolic solution the spectra exhibit three main absorption features: The $n-\pi^*$ (LUMO) transition (denoted as T_1) at a photon energy of 2.8 eV, which is dipole forbidden in the thermally stable, inversion-symmetric *trans* conformation of azobenzene, the strong $\pi-\pi^*$ (LUMO) transition (T_2) at 3.5 eV, and a broad absorption line at ~5 eV corresponding to higher $\pi-\pi^*$ transitions (T_3), where three sub-bands, marked by the vertical lines, can be discerned. The CF_3 marker group leads to a small overall red shift of the TF-Az6 spectrum by ~0.1 eV. The absorption spectra change gradually when an increasing amount of water is added to the ethanolic solution.[41] The T_2 transition at 3.5 eV fades, and an additional blue-shifted absorption maximum appears at 4.1 eV. Furthermore a slight red shift and splitting of the T_3 transitions occurs. These changes are attributed to aggregate formation in watery solution. The UV/vis absorption spectrum in the center part of Figure 5 was recorded for a 4 to 1 mixture of water to ethanol where aggregate formation is completed.

Corresponding to the absorbance (A) of the transmission spectra, the reflection spectra of the SAMs on Au/mica are plotted as $\log(R_{ref}) - \log(R_{SAM})$, where R is the particular reflectivity. The background of the reflection spectra increases toward higher photon energies. This stems from the modification of the reflectivity of the gold substrate by the thin molecular overlayer. As shown by the dashed line in Figure 5 the background can be qualitatively reproduced describing the SAM as a thin dielectric layer.[42,43] Here a layer with a thickness of 2.0 nm and a dielectric constant of $\varepsilon = 2.5$ has been assumed, while the optical constants of gold are taken from ref 44. In regions where the reflectivity of the gold substrate varies strongly with the wavelength, additional peaks arise. This occurs at 2.6 eV (the onset of the d -bands) and at 3.5 eV, accidentally coinciding with the $\pi-\pi^*$ (LUMO) absorption line. These substrate features, although rather weak, contribute significantly to the difference spectra, since the reflectivity changes only by 0.1−1% due to absorption of the azobenzene chromophores in the SAM. Considering this background the UV/vis spectrum of the SAM strongly resembles the absorption spectrum of the aggregates in watery solution. As for the latter the $\pi-\pi^*$ (LUMO) transition in the SAM is broadened and shows an additional contribution, blue-shifted by 0.6 eV relative to the T_2 absorption maximum in solution. Note that the absolute shift is comparable for TF-Az6 and Az6. The T_3 transition at ~5 eV shows in contrast a minor red shift of ~0.1 eV. Additionally the underlying peaks (marked by the vertical lines) are much better resolved. Compared to the T_3 absorption peak the T_2 transition is much weaker than in solution. The well-ordered SAMs on Au/mica showed no sizable signatures of photoisomerization upon irradiation at various photon energies in the UV range with photon doses of ~5 × 10^{20} photons/cm^2. In contrast for Az6-SAMs on semitransparent (nonwetting) gold films on quartz, we observed absorption changes in transmission in the order of 0.002 A,[41] comparable to those reported in refs 13 and 14.

Discussion

Structural Model of the SAM. Obviously the interaction between chromophores depends on the SAM architecture. Although NEXAFS spectroscopy probes the average orientation of all molecules with respect to the surface normal, it can provide insight into the intermolecular interaction for systems

(41) Freyer, W.; Brete, D.; Carley, R.; Schmidt, R.; Gahl, C.; Weinelt, M. *J. Photochem. Photobiol., A* **2009**, *204*, 102–109.
(42) Wakamatsu, T.; Toyoshima, S.; Saito, K. *J. Opt. Soc. Am., B* **2006**, *23*, 1859–1866.
(43) Orrit, M.; Möbius, D.; Lehmann, U.; Mayer, H. *J. Chem. Phys.* **1986**, *85*, 4966–4979.
(44) *Handbook of optical constants of solids*; Palik, E. D., Ed.; Academic Press, London, 1998; Vol. III.

with a high degree of orientation. This is the case for many SAMs of aromatic/aliphatic molecules linked via a sulfur headgroup to a gold surface.

For Az6 the 1*s* to LUMO transition dipole moment, which is perpendicular to the plane of the azobenzene chromophore in its *trans* configuration, is tilted by $\alpha = 76 \pm 3°$ with respect to the surface normal. This mean tilt angle α is very close to the value of $\alpha = 78°$ reported for biphenyls BP*n* adsorbed on gold with odd alkanethiol chain length $n = 1, 3, 5$.[45] Note that due to the phenoxy bridge Az6 has an odd chain length of $n = 7$. Even chain lengths result in somewhat smaller tilt angles of $\alpha \simeq 70°$.[45] It is, moreover, found that the tilt angles vary by a few degrees with the end group and the film structure.[9,46] For CN-BP1 and CN-BP2 smaller tilt angles of $\alpha \simeq 67°$ and 64° have been reported.[47] In a recent study molecular switches consisting of two biphenyl subunits linked by an azo group have been functionalized by a terminal sulfur group,[14] in the following referenced as BPA. These molecules also form well-ordered densely packed SAMs. The average tilt angles α of the π^* TDMs have been determined by NEXAFS to 73° and 68° for the biphenyl and azo moieties, respectively. As in the case of Az6 the similar tilt angles suggest the formation of a SAM with molecules preferentially in the *trans* configuration.

For fixed α the azobenzene moiety can still be rotated around the axis of the transition dipole moment perpendicular to the molecular plane. To further constrain the adsorption geometry either the tilt angle ϑ or the twist angle γ needs to be determined. From the $\sigma^*(C-CF_3)$ resonance we have deduced a tilt of the corresponding C−C axis with respect to the surface normal of $\vartheta = 30 \pm 6°$ and thus are able to derive also the twist angle $\gamma = 61 \pm 10°$ of the chromophore. There are only a few studies of aromatic SAMs where the molecular orientation has been determined to this extent. Fourier transform infrared spectra (FTIR) of X-BP0 yield tilt angles ϑ of 12°−20° depending on the end group X.[46] From a combination of FTIR and NEXAFS measurements a twist of $\gamma = 61 \pm 10°$ was determined for BP*n* = 1, 3, 5 resulting in a tilt of $\vartheta = 23 \pm 7°$.[45] The data evaluation and concomitant assumptions are rather involved in the FTIR experiments. In contrast, NEXAFS gives direct access to the orientation of the core to valence transition dipole moments. Most recently in a study of CN-BP1 the π^* resonances of the nitrile end group served as a marker to determine the twist angle γ to $50 \pm 3°$ resulting in a tilt of $\vartheta = 36°$.[47] The tilt and twist angles of Az6 and BPn molecules in SAMs are very similar. This suggests that the aromatic moieties arrange in an analog manner to optimize the interaction of their π electron systems.

Having examined in detail the average orientation of the adsorbed molecules, we now turn to their mutual arrangement and the resulting interaction among the chromophores within the SAM. AFM and STM measurements of Az6 on Au/mica show that the SAM forms a well ordered nearly rectangular lattice with two molecules per unit cell. Domains of different structures have been found with the two molecules either close together or evenly spaced. The respective unit cells, although, have the same dimensions. For the basis vectors, values of $a = 6.05$ Å, $b = 7.8$ Å[16] and $a = 6.3$ Å, $b = 8.2$ Å[17] are reported, slightly smaller than those for the two biphenyls linked by an azo group ($a = 6.5$ Å, $b = 8.9$ Å).[13] For the two phases of Az6 a sandwich herringbone and a herringbone structure have been suggested.[16] Similar structures have been proposed for SAMs of Az10[48] and Az11.[19] However, none of these studies determined details of the molecular orientation.

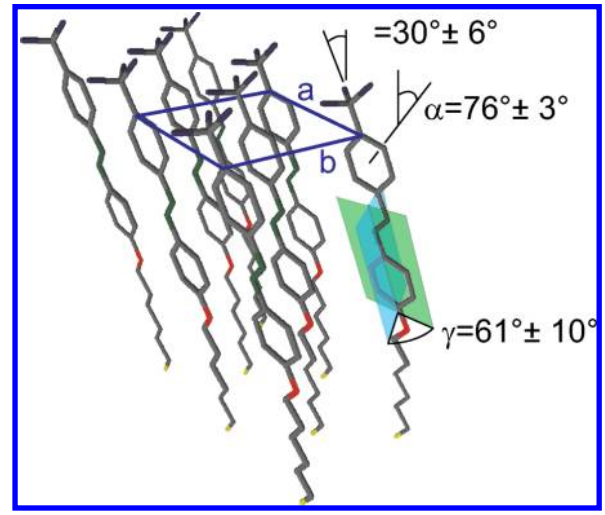

Figure 6. Structural model of the SAM of the azobenzene-functionalized alkanethiols. The molecules are located at the corners and in the center of the rectangular unit cell with lattice vectors $a = 6.05$ Å and $b = 7.80$ Å.

The structure model used for the calculations is depicted in Figure 6. For simplicity our model assumes equal orientation of the two azobenzene chromophores in the unit cell. We note that the two angles α and ϑ fix the orientation of the chromophore with respect to the surface normal, but the molecule may still be moved on a cone. For two molecules per unit cell this allows for different herringbone-like arrangements of the chromophores in the SAM as will be taken care of in the modeling of excitonic coupling.

Excitonic Coupling among the Chromophores. The azobenzene end group attached to the alkyl chain is efficiently decoupled from the metal substrate. This has been established by measurements of charge transfer dynamics in SAMs carrying a nitrile end group,[49] and we also verified this by recent autoionization measurements of TF-Az3, TF-Az6, and TF-Az10. Therefore the optical properties of the chromophores in the SAM will be little influenced by the substrate but can be altered by lateral interactions among the chromophores. This is in contrast to the recently investigated azobenzene and tetra-*tert*-butyl-azobenzene molecules on Au(111), where adsorbate−substrate interaction dominates over intermolecular coupling and is even made responsible for optical induced switching.[12,50,51]

To describe the interaction between the chromophores and simulate the influence of excitonic coupling on the UV/vis spectrum of the azobenzene-alkanethiol in the densely packed and well-ordered SAM, we follow the concept of exciton band

(45) Rong, H.-T.; Frey, S.; Yang, Y.-J.; Zharnikov, M.; Buck, M.; Wühn, M.; Wöll, C.; Helmchen, G. *Langmuir* **2001**, *17*, 1582–1593.
(46) Kang, J. F.; Ulman, A.; Liao, S.; Jordan, R.; Yang, G.; Liu, G.-Y. *Langmuir* **2001**, *17*, 95–106.
(47) Ballav, N.; Schüpbach, B.; Dethloff, O.; Feulner, P.; Terfort, A.; Zharnikov, M. *J. Am. Chem. Soc.* **2007**, *129*, 15416–15417.
(48) Wang, R.; Iyoda, T.; Jiang, L.; Tryk, D. A.; Hashimoto, K.; Fujishima, A. *J. Electroanal. Chem.* **1997**, *438*, 213–219.
(49) Neppl, S.; Bauer, U.; Menzel, D.; Feulner, P.; Shaporenko, A.; Zharnikov, M.; Kao, P.; Allara, D. *Chem. Phys. Lett.* **2007**, *447*, 227.
(50) Comstock, M. J.; Levy, N.; Kirakosian, A.; Cho, J.; Lauterwasser, F.; Harvey, J. H.; Strubbe, D. A.; Frechet, J. M. J.; Trauner, D.; Louie, S. G.; Crommie, M. F. *Phys. Rev. Lett.* **2007**, *99*, 038301.
(51) Hagen, S.; Kate, P.; Leyssner, F.; Nandi, D.; Wolf, M.; Tegeder, P. *J. Chem. Phys.* **2008**, *129*, 164102−1–8.

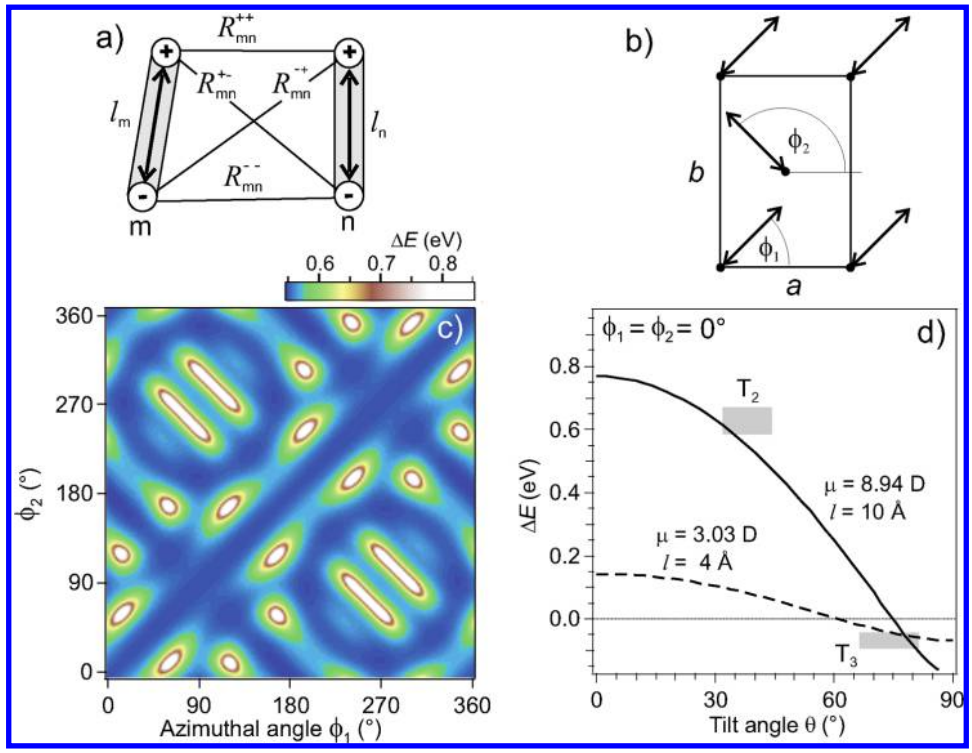

Figure 7. Extended dipole model (EDM): (a) Transition dipoles m and n of length l and charge separation R_{mn}. (b) Top view showing the orientation of optical transition dipole moment μ relative to the lattice. The angles ϕ_1 and ϕ_2 define the azimuthal orientation of the two transition dipole moments in the unit cell. (c) False color plot of the calculated spectral shift of the T_2 dipole transition with respect to the azimuthal orientation ϕ_1 and ϕ_2 for fixed tilt angle $\theta = 38°$. (d) Calculated spectral shifts ΔE for the T_2 (solid line) and T_3 transition (dashed line) as a function of the tilt angle θ of the corresponding optical transition dipole moment. The gray horizontal bars mark the expected coordinates of the dipole moments $\mu(T_2)$ and $\mu(T_3)$: The energy shift of the transition dipole moments is taken from UV/vis spectroscopy, and the angle θ is determined by combining the orientation deduced from the NEXAFS measurements and the orientation of the optical dipole moment calculated via TD-DFT. The extension of the bars represents the experimental errors.

formation.[52] Since the extent of the chromophores is of the same size as the intermolecular distance, we describe the excitonic coupling within the SAM in the framework of the extended dipole model (EDM), which has been applied successfully to various aggregate systems.[23,53] The transition dipole moment is approximated by a pair of charges separated by a certain distance l. For equal molecules, the matrix element describing the interaction between transition dipole moments at molecules m and n is then approximated by[53]

$$J_{mn} = \frac{|\mu|^2}{4\pi\varepsilon_0\varepsilon l^2}\left(\frac{1}{R_{mn}^{++}} + \frac{1}{R_{mn}^{--}} - \frac{1}{R_{mn}^{+-}} - \frac{1}{R_{mn}^{-+}}\right) \qquad (3)$$

Herein μ denotes the transition dipole moment of the respective absorption line. ε_0 and ε are the dielectric permeability and the dielectric constant. R_{mn} stands for the distance between the charges constituting the extended dipoles as sketched in Figure 7a.

For a two-dimensional ordered lattice of equivalent molecules and in the limit of large aggregates only the excitonic mode with all transition dipoles in-phase contributes to the optical absorption spectrum. For a herringbone structure an additional mode with smaller but finite total transition dipole moment exists, where the molecules of the two species are excited out-of-phase. To calculate the energy shift of the absorption lines for the two lowest optical transitions of TF-Az6 and Az6 SAMs, we take as input the structure with the tilt and twist angles determined from NEXAFS spectroscopy together with the lattice parameters determined by Wolf, Jaschke et al.[16] The transition dipole moments $\mu(T_2) = 8.94$ D and $\mu(T_3) = 3.03$ D of the T_2 and T_3 optical bands and their orientation with respect to the C−CF_3 axis are taken from our TD-DFT calculations. Guided by the extent of the π-electron system along the respective directions, the lengths of the dipoles l of the T_2 and T_3 transitions are taken to be 10 Å and 4 Å, respectively. The calculations include the interaction with all neighbors in a lattice consisting of 50 × 50 unit cells.

To investigate the interaction between neighboring transition dipoles we varied their azimuthal angles, ϕ_1 and ϕ_2, in Figure 7b, independently. In Figure 7c the angular dependence of the spectral shift is presented for the T_2 transition with a dipole length of $l = 10$ Å in a false color plot. Corresponding to $\vartheta = 30°$ the tilt angle of the optical transition dipole moment is taken as $\theta = 38°$. The areas of large spectral shifts (white) correspond to angle combinations where the partial charges of the extended dipoles approach each other closely. Hence these orientations are forbidden for steric reasons. As seen from the dark diagonal stripes, all combinations of equal azimuthal orientation for both molecules in the unit cell represent configurations, where the intermolecular coupling, especially the excitonic coupling, is small ($\phi_1 = \phi_2$). The same holds along the path where the molecules rotate exactly counterclockwise ($\phi_1 = 180° - \phi_2$). In these configurations the excitonic band shift for large aggregates amounts to ~0.55 eV. This is of the same order of magnitude as the experimentally observed value of 0.6−0.65 eV for the blue-shifted absorption maximum and strongly

(52) Davydov, A. S. *Theory of Molecular Excitons*; Mc Graw-Hill: New York, 1962.
(53) Kato, N.; Yuasa, K.; Araki, T.; Hirosawa, I.; Sato, M.; Ikeda, N.; Iimura, K.-I.; Uesu, Y. *Phys. Rev. Lett.* **2005**, *94*, 136404−1–4.

supports that the interaction among the transition dipoles can very well describe the spectral shift of the T_2 transition in the UV/vis spectra. The calculated spectral shift remains >0.5 eV, even if we vary the position of the second transition dipole moment within the unit cell and if we allow for differing orientations of the two molecules in the range compatible with the experimentally determined average orientation. Therefore we expect similar energetic shifts for the different phases reported for Az6 SAMs.

To evaluate the spectral shifts as a function of the tilt angle of the dipole moments θ with respect to the surface normal we assume $\phi_1 = \phi_2$, where the influence of steric hindering and repulsive dipole−dipole interactions is small. The respective shifts of the dipole moments $\mu(T_2)$ and $\mu(T_3)$ of transitions T_2 and T_3 are depicted in Figure 7d.[54] Overall the energy shift of the T_3 transition is much smaller because its smaller transition dipole moment enters eq 3 quadratically. The gray horizontal bars mark the measured energy shift of the dipole transitions T_2 and T_3 and the angular ranges for θ which are consistent with the molecular structure determined from NEXAFS, i.e. the angles α and ϑ. Given the rather simple extended dipole model and the complex structure of the SAM, experimental and calculated shifts agree well. Small corrections may stem from the additional static dipole interactions resulting from a change of the charge distribution in the excited state which have been neglected here.[53] However, even the present level of the modeling unambiguously establishes that the shift of the optical transitions is a clear signature of the interaction between the transition dipoles. The T_2 and T_3 transitions are blue- and red-shifted and form accordingly H and J aggregates, respectively, in both the watery solution and the SAM. For the T_2 transition the model reproduces only the position of the blue-shifted maximum, since it does not include the effect of defects and the coupling to nuclear motion.

For BPA-SAMs on gold with lattice parameters and a molecular orientation comparable to Az6, high switching yields have been reported.[13,14] Taking the given SAM structure and assuming the same transition dipole moment as that for Az6, the extended dipole model predicts a blue shift of ∼0.5 eV for large well-ordered SAM areas of BPA.

Concerning the photoisomerization within a well-ordered SAM, the question arises if the optical excitation resides long enough at one molecule that the photoisomerization process is triggered and the chromophore is decoupled from its neighbors. Eisfeld et al. calculated absorption spectra for H-aggregates corresponding to the T_2 absorption line taking explicitly into account coupling to vibrational degrees of freedom.[55] They came to the conclusion that if the energetic shift of the H-band exceeds the width of the monomer spectrum, energy transfer to vibrations is suppressed since the excitation energy is delocalized faster than it can be transferred to the nuclear coordinate. An energy change of 0.65 eV corresponds to a delocalization time on the order of 1 fs and exceeds the width of the monomer spectrum of 0.5 eV. As optical excitation of this π to π^* transition triggers the *trans* to *cis* isomerization of the azobenzene in solution, photoswitching in the SAM is ineffective. Since the isomerization reaction takes ∼1 ps,[56,57] we believe that in addition to steric hindrance this delocalization of the excitation on the femtosecond time scale constitutes a strong constraint to photoswitching within well-ordered SAMs. In the vicinity of structural defects, e.g. also *cis* isomers, where the excitonic coupling is weakened, the isomerization probability might increase again. Although not observed in the present case, this cooperative effect could promote the formation of switched domains[13,14] and explain the data obtained from rough gold surfaces.

Conclusions

On the basis of NEXAFS measurements, UV/vis spectroscopy, and DFT calculations, we have developed a consistent picture of the geometric structure and optical properties of the photoswitch azobenzene attached as an end group in a hexanethiol SAM. The orientation of the molecules in the SAM follows the self-assembly principles of aliphatic-aromatic SAMs and is quite similar to that of the recently investigated biphenyls.[9,47] Attaching a trifluoro-methyl marker to the azobenzene end group, we can determine the molecular orientation to a large extent and deduce the tilt and twist angles as 30 ± 6° and 61 ± 10°. On the basis of the geometric structure the 0.6−0.65 eV blue shift of the T_2 (π to π^* (LUMO)) and 0.05 eV red shift of the T_3 (π to π^* (LUMO+n)) transitions is qualitatively described by an extended dipole model.[23] This demonstrates formation of H and J aggregates and the importance of excitonic coupling among the azobenzene π systems. We conclude that strong delocalization in the densely packed layer quenches the optical excitation on an ultrafast time scale and thereby impedes molecular switching in the SAM.

This detailed insight into the intermolecular coupling will help to design structures with proper functionality. While dilution of the switch has been recently shown to restore functionality,[21] many applications ask for switching a larger fraction of molecules.[13] Here excitonic coupling may open a new perspective in imitating light harvesting complexes and controlling excitation flow in a SAM by tuning the optical properties of the chromophores.

Acknowledgment. Support by the Deutsche Forschungsgemeinschaft through Sfb 658 - Elementary Processes in Molecular Switches at Surfaces - is gratefully acknowledged. We thank Peter Feulner for valuable discussions and the BESSY staff, in particular Matthias Mast and Olaf Schwarzkopf for technical support.

Supporting Information Available: Complete ref 28. This material is available free of charge via the Internet at http://pubs.acs.org.

JA903636Q

(54) The energetic shift as a function of θ changes by less than 50 meV for other angle combinations $\phi_2 = 180-\phi_1$.

(55) Eisfeld, A.; Briggs, J. S. *Chem. Phys.* **2006**, *324*, 376–384.
(56) Nägele, T.; Hoche, R.; Zinth, W.; Wachtveitl, J. *Chem. Phys. Lett.* **1997**, *272*, 489–495.
(57) Fujino, T.; Arzhantsev, S. Y.; Tahara, T. *J. Phys. Chem. A* **2001**, *105*, 8123–8129.